A 3D Crust and Upper-Mantle Velocity Model for the Gulf of California Region from Surface Waves

F. Di Luccio[1], R. W. Clayton[2] and P. Persaud[2]

Submitted to J. Goephys. Res. March 1, 2006

[1]Istituto Nazionale di Geofisica e Vulcanologia, Via di Vigna Murata 605, 00143, Rome, Italy. Phone 0039-06-51860561, diluccio@ingv.it.

[2]California Institute of Technology, Seismological Laboratory, MS 252-21, Pasadena, CA 91125. Phone 001-626-395-6909, clay@gps.caltech.edu and ppersaud@gps.caltech.edu.

Abstract

We use Rayleigh wave group velocity dispersion measurements from 30 local earthquakes to determine the crust and upper-mantle shear-wave velocity for the Gulf of California region. The 3D model has its best resolution in the Gulf itself and deteriorates toward the edges due to a lack of station coverage. The results show shallow slow anomalies associated with the well-developed rifting in the southern and central part of the Gulf (Alarcon and Pescadero basins, respectively), and slow anomalies associated with the sedimentary basins. There is a significant mid-Gulf fast velocity that is spatially coincident with the active volcanic region on the Baja peninsula. The results show that the diffuse rifting in the northern gulf extends into the upper mantle, in contrast to the southern Gulf where both the rifting and velocity anomalies tend to be in narrow zones. Consequently, the rifting process is interpreted as done by flow across a broad zone in the lower crust. A thinning in the crustal thickness is found from north to south beneath the Gulf, with a shallower Moho in the eastern side underneath the Sonora and Sinaloa regions.

Introduction

The Gulf of California is one of only a few easily-accessible, newly forming ocean basins where seafloor spreading is still not fully established. At the southern margin of the Pacific-North America plate boundary, the Gulf of California extends ~1400 km from southern California to the spreading mid-ocean ridge system of the East Pacific Rise. East-west extension in the Gulf of California appears to have started approximately 12 Ma when the subduction of the lithosphere along the western margin of Baja California ceased [*Lonsdale*, 1989] and a series of basins and long transform faults were produced. About 6Ma the Pacific-North America plate margin was then shifted about 250 km inland roughly parallel to the coast line [*Oskin et al.*, 2001]. This shear zone is thus characterized by basins, orthogonal or oblique to the en echelon-type transform faults, with most of the active basins located where extension is predominant. Tectonic complexities are related to the size and re-orientation of these basins in time. Some of the basins especially at the mouth of the Gulf, including the Guaymas basin, also show seamounts, whereas in the central and northern Gulf magmatism is represented as dike or sill intrusions into young sediments [*Lonsdale*, 1989]. The amount of volcanism along the transform faults is poorly determined due to the lack of samples. The basins become deep from north to the south, with the northern ones showing the thicker sedimentary blanket [*Lonsdale*, 1989].

Seismological studies confirm the complexity in the pattern of spreading because of strong lateral variations in the crustal and upper-mantle structure beneath the Gulf [*Thatcher and Brune*, 1973]. Crustal deformation beneath the Gulf ranges from classic ridge-transform structures in the south to diffuse deformation in the north, where a large number of shallow small-offset normal faults exist [Persaud *et al.*,2003].

Various schools of thought exist on what type of crust underlies the Gulf, whether crustal composition and thickness varies along strike and what the possible causes of these inferred differences might be. Seismic refraction studies in the northern Gulf require a crustal structure that is similar to that found in the continental borderland of Southern California and a crustal thickness of ~20-25 km [*Phillips,* 1964]. More recent work also provides large values of crustal thickness for the northern Gulf and supports a crustal structure in the northern Gulf that is not typical

of normal oceanic crust [*Gonzales et al.,* 2005]. Along a profile at ~31°N latitude, Moho depth estimates from P-to-S converted phases increases from 33±3 km near the Pacific coast of Baja California to 40±4 km beneath the western part of the Peninsular Ranges batholith [*Lewis et al.,* 2001]. The crustal thickness then decreases rapidly across the eastern Peninsular Ranges and Main Gulf Escarpment to a fairly uniform thickness of (15-18)±2 km within and on the margins of the northern Gulf [*Lewis et al.,* 2001]. This eastward thinning of the crust is also confirmed for the entire Baja California peninsula by a recent study by *Persaud et al.* [2005], where crustal thickness variations in the Gulf of California region are obtained from receiver functions, using teleseismic data recorded at the NARS-Baja array. They find a thinning of the crust from the western side of the Baja California peninsula towards the Gulf as that is consistent with the compositional boundary going from southern California to the tip of Baja California and separating the western and eastern Peninsular Ranges Batholith (PRB) [*Langenheim and Jachen*, 2003]. Thinner crust is also found beneath the southernmost stations (NE76, NE77, NE79 in Figure 1) compared to the crustal thickness for the northern stations (NE71, NE72, NE73, NE74 and NE75 in Figure 1) which ranges from 28 to 38 km.

Furthermore, from the analysis of deep seismic profiles and new gravity data, *González-Fernández et al.* [2005] constrain the crustal depth below the upper Delfín and the Tiburón basins in the northern Gulf of California. They find the crust progressively thickens outwards east (Sonora region) and west (Baja California peninsula); a crustal thickness of 19 km has been estimated underneath the coastline, whereas the crust goes up to 14 and 17 km in the upper Delfín and the Tiburón basins respectively and thickens down to 19.5 km in between the two basins [*González-Fernández et al.,* 2005].

Regional waveforms propagating through the upper mantle in the Gulf are 5-10% slower than in normal mantle [*Thatcher and Brune,* 1973]. In the uppermost 200 km of mantle beneath the Gulf, the S-wave velocity is 6-8% slower than in the Preliminary Reference Earth Model, similar to other ridges/rifts (e.g., the East Pacific Rise and Red Sea rift) [e.g. *Ritsema and van Heijst,* 2000]. It is estimated that the margins of the Gulf have undergone at least 255±10 km of horizontal separation of the upper crust [*Oskin et al.,* 2001] and the mantle looks seismically similar to that found at a mid-ocean ridge. However, seafloor-spreading magnetic lineations extend only as far north as the Pescadero basin [*Larson et al.,* 1972].

Regional constraints on crust and upper mantle velocities are important for studies of lithospheric structure and deformation. This is particularly true in target areas like the Gulf of California, where the scientific community hopes to gain a fundamental understanding of lithospheric rupture. Thus far, the basic lithospheric properties of the Gulf and its margins remain unresolved. Here we present a surface wave dispersion study of regional earthquake data recorded by the NARS-Baja array, a set of 14 broadband seismic stations surrounding the Gulf of California and the 5 broadband stations of the Red Sismologica de Banda Ancha (RESBAN network) (Figure 1). Surface wave studies are key to building 3D regional velocity models from a sparse seismic network because they provide horizontal sampling through the model with broad beams, and because they utilize the dispersive characteristics of the largest amplitude and mostly easily recognizable waves recorded in seismograms to determine the first-order velocity structure along event-station paths. In this study, we analyze Rayleigh waves from regional earthquakes to create a 2D map of the group velocities in the region, which are then be used to determine the 3D structure. Noticeable differences in the group velocities are found for the northern and southern Gulf of California as well for the Peninsular Range and

adjacent basins. Due to the fact that the NARS-Baja array straddles the plate boundary, we are able to make additional first-order comparisons of the crust on opposite sides of the conjugate margins. This paper contributes to the understanding of the Pacific-North America boundary deformation by defining the crustal and upper mantle structure beneath the Gulf of California and its western and eastern confining regions.

Data analysis and model construction

We use a standard procedure [v*an der Lee and Federiksen*, 2005] to determine the 3D velocity model from surface waves. The first step is to determine the group-velocity dispersion curves for the surface wave paths that cross the model. These are then converted to maps of group velocity by a tomographic inversion, and finally, the dispersion relation at each x-y point in the model is inverted for the vertical velocity.

We derive the group-velocity dispersion from regional earthquake data recorded by the NARS-Baja and RESBAN arrays. We use regional earthquakes because they are most sensitive to the structure in the Gulf itself, and we use group velocity because it is not strongly sensitive to the earthquake locations for their initial phase. Dispersion data from this study only included the vertical (Rayleigh) component seismograms, and the selected periods are those along the smoothest part of the spectral amplitude curve. We did not use Love waves because for most paths it was difficult to isolate the fundamental mode for these waves.

Events with magnitudes greater than 4, within a depth range of 5-33 km and distance range of 2°-15° were selected from the NEIC bulletin. The locations of the earthquakes and the relative source-to-receiver paths are shown in Figure 1 and listed in Table 1. An example of a regional earthquake recorded at the NARS-Baja and RESBAN broadband stations is shown in Figure 2, where the frequency content of the waveform vertical components clearly depend on the propagation path. Dispersion curves of Rayleigh waves are computed in the period range 5-100 s, with 75% of the measures being in the band 5-50 s. The period range of each dispersion curve depends on the magnitude of the earthquake and the source to receiver distance, with longer periods from larger events being better recorded at longer distances. Group velocities of the Rayleigh wave fundamental mode were computed using a Multiple Filter Analysis (MFT) technique [*Dziewonski*, 1969], with a phase matched processing by MFT [*Herrin*, 1977] to isolate the fundamental mode wave. We use a program by *Herrmann and Ammon* [2002] which provides a fast and efficient method of analyzing multiply dispersed signals. To measure group velocity from seismogram vertical component, the quality of the recording has first been evaluated in terms of signal to noise ratio, to avoid noise sources contributing to the energy that arrives at the same time as the surface wave. A cause of error in the dispersion curve determination is due to mis-locations, with longer source-receiver paths being less sensitive to epicentral location errors than shorter paths. To minimize this type of error we use a minimum path length of 300 km. After de-meaning and de-trending, the instrumental response has been deconvolved from the seismograms in order to obtain displacements. The measure technique is extensively described in [*Herrmann,* 1973].

Measured group velocities along each path range from 2 to 5 km/s. We show in Figure 3 some examples of dispersion curves for different paths at three sample stations (see Figure 1 for the station location). The slopes of the group velocity curves range from very steep to smooth. In general, the characteristics of the 3 sets of group velocity curves are very different (Figure 3). The observed group velocities are faster for the station in Sonora (NE80) than for stations in Baja. Although the two events at the mouth of the Gulf (eq1 and

eq12) are very closely located and their focal mechanisms are very similar (Figure 1), the group velocities along similar paths (i.e. NE71 in Figure 3), were always lower for eq1 than for event eq12. This is likely related to the fact that event eq1 is closer to a ridge than eq12. The maxima of the group velocities are less than 4 km/s for all the shown paths except those for eq10 and eq11 at the stations NE71 and NE80. In addition, for events eq10 and eq11 the minimum group velocity is low at stations south of 29°N (NE79 in Figure 3) compared to the stations to the north. In contrast, the two events that occurred close to the Rivera Transform Fault (eq8 and eq20) gave almost identical dispersion curves for a number of paths. Interesting features can be observed for most of the paths in Figure 3. For example, at periods between 20 and 50 s the curve of the fundamental mode is not smooth as for shorter periods, which likely reflects structural variations in the upper mantle.

We use the dispersion curves computed along specific paths to create a 2D map of the group velocities in the Gulf of California region. We divided the area into columns spaced at 0.2° in the Gulf of California where the path coverage is good and spaced at 1° outside the area of crossing paths (Figure 4). Each column is initially defined with a starting velocity model in which the crustal layers are taken from receiver functions studies by *Ichinose et al.* [1996], *Lewis et al.* [2002], *Persaud et al.*, [2005], (green dots), or from a reflection study by *González-Fernández et al.* [2005] (blue dots). Outside the well-sampled area, CRUST2.0 [*Bassin et al.*, 2000] is used as the reference model. For all the columns, IASP91 is used as the starting model for the mantle down to 500 km. The dispersion measurements along the paths are converted to a map of the group velocity by standard back-projection tomography using kernels that vary in off-path width with the square-root of the period [v*an der Lee and Frederiksen*, 2005]. Once we have the group velocities for each grid node then we invert these curves to get the velocity structure. A linearized method is used in the 1D inversion with a starting velocity model consisting of homogeneous horizontal layers [*Herrmann and Ammon*, 2002]. The inversion procedure consists of taking a starting velocity model, calculate the dispersion curve from this starting model, and compare with the observed. If they agree within the errors, we are done, otherwise we refine the starting model iteratively until it fits the data. We first invert for the thickness then we estimate velocity versus depth for different crustal types. During the inversion, the Vp/Vs ratio for each layer is fixed, while density is obtained from the P-wave velocity.

We inverted Rayleigh group velocities which were smooth at both short and long period. There is no weighting of any particular layer in the inversion to allow the gross structure to be apparent. Iterations are controlled to avoid spurious low velocity zones in the model and if this happens, the layer thicknesses are changed and another inversion is run. The final model is the one that fits both the observations and the local structure from other studies. For each fit, the velocity dispersion mean error and its standard deviation error are given. During each iteration the standard deviation between the observed and predicted models should reach a point where the change in the model is negligible (the model converges). A stochastic damped least squares inversion includes a damping factor that limits the size of model variations between each iteration. The level of the damping factor affects how fast the model converges and the reduction in the standard deviation between the observed and predicted values. We used a damping factor of 10 because it gives the most stable results with a reasonable (between 10 and 20 as a maximum) number of iterations.

The determination of the predicted dispersion curves is affected by errors due to noise, scattering, and in earthquake origin times. These errors could decrease the accuracy

of the shear-wave velocity and crustal thickness during the inversion, but we think we minimized their impact, by carefully selecting the data used. In this model we also neglected the effects of anisotropy in favor of determining that main lateral variations in velocity.

The results for velocity are summarized in Figure 5, where the central panels show the standard models at three locations in the Gulf while the right panels show the final models from the inversion. The inversion puts in significant low velocity zones. The left panel shows a comparison of predicted (solid lines) and the observed (dots) dispersion curves. The details are not fitted by this regional model, but in this analysis we attempt to fit the short periods (< 40 s) and get the best trend at longer periods. In the final models at 23°N in Figure 5 a very pronounced inversion in the shear velocity is found and it corresponds to the southernmost Gulf.

Results

The shear wave velocity model is presented in Figure 6a, in which a set of cross sections crossing the main ridge segments in the Gulf is shown. The southernmost image (E profile) that crosses the Alarcon rise shows a strong low velocity zone down to 30 km beneath Baja California which shallows eastward beneath the Alarcon basin. In the same two cross-section fast velocity zones are evident separated by a thin slow velocity. The D image (Figure 6a) shows the asthenosphere image of the Pescadero ridge segment (PB in Figure 4), where the anomalous shear-wave velocities are 3 km/s or less. The strong anomaly is coincident with the active ridge. The C transect to the north (Figure 6a) crosses the Guaymas basin, GB and has also slow velocities. Cross-section B, in contrast, has a more laterally diffuse, but still pronounced zone of slow velocities. In the region spanned by cross-sections B and C the ridge segments are short while the transform segments are relatively long, and this is probably reflected in the velocity anomalies. In the northernmost segment (A in Figure 6a) across the Delfín basin (DB in Figure 4) , the slow anomaly is shallow and spread across the entire Gulf with no particular focus zone. The main feature of Figure 6a is that the slow velocity zone shallow from south to north, according to the shallowing of the basins.

In Figure 6b, a systematic grid of images dissecting the Gulf region is presented, showing NW-SE cross-sections along Baja peninsula, the Gulf of California, Sonora and Sinaloa regions respectively. The main feature beyond the ridge image described above is the slow region under the mid-peninsula (28°N) and the fast region underneath northeastern part of the Gulf (Sonora, 30°-31°N) and the southern tip of Baja California (23°N). Shear-wave velocities reach ~ 4.5 km/s beneath Baja California and are in the range 4.2 – 5.4 km/s in Sinaloa and Sonora respectively.

In Figure 6c, three ~1200 km long profiles are plotted: the western profile (W) along the Baja California peninsula, the mid-profile (M) along the Gulf axis and eastern profile (E) traversing the Sonora and Sinaloa regions. The main features in Figure 6c are: the important low velocity zones in the central part of M and E profiles and the fast lithosphere coming up at ~ 30 km in depth beneath Sonora.

In Figure 7, we show maps of sediment (top) and crustal (bottom) thickness in the starting and final models. The initial sediment models were specified from CRUST2.0, while the initial crustal thickness (Moho depth) was determined CRUST2.0 and from receiver functions [*Persaud et al.*, 2005] when available. The final models are the result of inverting the dispersion curves starting with the initial models. The sediment thickness map primarily shows the major basins in the Gulf (north to south: Wagner, Guaymas, and Alarcon basins). The large low velocity anomaly on the southwestern side of the Baja Peninsula is coincident with the Magdalena sedimentary fan,

but it is also located at the boundary of the model resolution. Deep sediments are found in the Guaymas basin, northeast of Baja California and in the Pescadero and Alarcon basins (PA and AB in Figure 4), while shallower sediments are found in the northern Gulf and at latitude 25°-26°N.

The crustal thickness shows the south to north thickening that was also evident in the receiver function results [*Persaud et al.*, 2005], but it indicates that the trend is less gradual and changes by about 5 km at latitude 27°N. A thick crust has found at the very northern of the Gulf. The localized thick crust in Sonora at latitude 28°N may be an artifact and the crustal thickness beneath Sonora and Sinaloa is globally shallower than along the Peninsula.

Shear-wave velocity maps are shown in Figure 8, in which we divide the crust in three layers according to Crust 2.0 [*Bassin et al.*, 2000] and we compare the initial velocities to the ones obtained from the inversion. The main feature is the low velocity zone imaged in the upper crust and upper mantle beneath the Guaymas, Pescadero and Alarcon basins and southwest of Baja in the Magdalena fan. Low velocities observed in the upper crust beneath the northern Gulf become faster as we go deeper into the upper mantle. Relatively fast shear velocities are found in the middle and lower crust beneath the Isla Angel de la Guarda and the Guaymas basin. In both Figure 7 and 8, it should be kept in mind that the resolution of the inversion is strictly dependent on the source-to-receiver path coverage (grey lines in Figure 1 and Figure 4).

Discussion and Conclusions

One of the issues with rifting in the Gulf is the apparent change in style from south to north. The results shown here indicate that in the south, the upwelling upper-mantle/asthenosphere is localized and in the farthest south (Alarcon Basin) it is coincident with the location of the ridge. As you move to the north, the slow anomaly in the mantle spreads across the whole width of the Gulf. At the same time the crust becomes thicker. This favors a model in which the rifting process is done by flow across a broad zone in the lower crust. In the case of the Guaymas Basin (profile C in Figure 6a) the focused zone of the asthenosphere appear to the west of the ridge, possibly indicating that the ridge will move in that direction in the future, as it has done in the past.

Another issue in the Gulf is the role of the remnant slab in the rifting process. In this study we see no evidence for a slab in the upper mantle. However, the surface waves in the periods we use in this study would not be particularly sensitive to a localized slab in the mantle.

Whether the crust is mainly oceanic, continental or transitional in composition, we have found a thinning of the crustal thickness from north to south beneath the Gulf and from west to east, but we don't have evidence for a symmetrical crustal thinning as deduced from other studies [*Couch et al.*, 1991]. The Moho depth underneath the Sonora and Sinaloa regions is generically shallower than beneath Baja and the Gulf. The importance of the sedimentary coverage is also evidenced in our results as with previous studies.

In this paper a 3D velocity model is produced for the Gulf of California and surrounding regions. A 1D velocity model is easily derivable from our structural model for each point of interest and reliable on earthquake locations and geodynamic modeling. The model is available at the site: http://www.data.scec.org/NARS-Baja/

Acknowledgements

This research was partially supported by NSF award EAR-0405437. We thank our collaborators at Utrecht and CICESE for their effort in running the NARS-Baja array.

References

Bassin, C., G. Laske, and G. Masters (2000), The current limits of resolution for surface wave tomography in North America, in EOS Trans. AGU, F897, 81.

Couch, R. W., G. E. Ness, O. Sanchez-Zamora, G. Calderon-Riveroll, P. Doguin, T. Plawman, S. Coperude, B. Huehn, and W. Gumma (1991), Gravity anomalies and crustal structure of the gulf and peninsular province of the Californias, American Association of Petroleum geologists Memoir, 47, 24–45.

Dziewonski, A., S. Bloch, and M. Landisman (1969), A technique for the analysis of transient seismic signals, Bull. Seism. Soc. Am., 59(1), 427–444.

González-Fernández, A., J. J. Dañobeitia, D. Córdoba, L. A. Delgado-Argote, R. Carbonell, and R. Bartolomé, (1999), Estructura de la litosfera en el Alto Golfo de California a partir de datos de sísmica de reflexión, gran ángulo y gravimetría, GEOS Unión Geofis. Mex., 19, 219.

González-Fernández, A., J. J. Dañobeitia, L. A. Delgado-Argote, F. Michaud, D. Córdoba, and R. Bartolomé, (2005), Mode of extension and rifting history of upper Tiburón and upper Delfín basins, northern Gulf of California, J. Geophys. Res., 110, doi: 10.1029/2003JB002941.

Herrin, E., and T. Goforth (1977), Phase-matched filters; application to the study of Rayleigh waves, Bull. Seism. Soc. Am., 67(5), 1259–1275.

Herrmann, R. B. (1973), Some aspects of band-pass filtering of surface waves, Bull. Seism. Soc. Am., 63(2), 663–671.

Herrmann, R. B., and C. J. Ammon (2002), Computer programs in seismology - surface waves, receiver functions and crustal structure, Saint Louis University, http://www.eas.slu.edu/People/RBHerrmann/ComputerPrograms.html.

Ichinose, G., S. Day, H. Magistrale, and T. Prush, (1996), Crustal thickness variations beneath the Peninsular Ranges, southern California, Geophys. Res. Lett., 23(22), 3095-3098.

Langenheim, V. E., and R. C. Jachens (2003), Crustal structure of the Peninsular Ranges batholith from magnetic data: Implications for Gulf of California rifting, Geophys. Res. Lett., 30(11), doi:10.1029/2003GL017159.

Larson, P. A., J. D. Mudie, and R. L. Larson, (1972), Magnetic anomalies and fracture zone trends in the Gulf of California, Bull. Geol. Soc. Am., 83, 3361-3368.

Lewis, J. L., S. M. Day, H. Magistrale, R. R. Castro, L. Astiz, C. Rebollar, J. Eakins, F. L. Vernon, and J. N. Brune (2001), Crustal thickness of the peninsular ranges and gulf extensional province in the Californias, J. Geophys. Res., 106(B7), 13,599–13,611.

Lonsdale, P., (1989), Geology and tectonic history of the Gulf of California, in Winterer, E. L. Hussog, D. M., and Decker, R. W., eds., The Eastern Pacific Ocean and Hawaii: Boulder, Colorado, Geolog. Soc. Of Am., vol. N.

Oskin, M., J. Stock, and A. Martin-Barajas (2001), Rapid localization of Pacific-North America plate motion in the Gulf of California, Geology, 29(5), 459–462.

Persaud, P., X. Pérez-Campos and R. W. Clayton (2005), Crustal thickness variations in the margins of the Gulf of California from receiver functions, submitted to Geophys. J. Int.

Persaud, P., J. M. Stock, M. Steckler, A. Martin-Barajas, J. B. Diebold, A. Gonzales-Fernandez, and G. S. Mountain (2003), Active deformation and shallow structure of the Wagner, Consag and Delfín basins, Northern Gulf of California, Mexico, J. Geophys. Res., 108(B7), doi:10.1029/2002JB001937.

Phillips, R. P. (1964), Seismic refraction studies in gulf of California, in Marine Geology of the Gulf of California, edited by T. van Andel and G. G. Shor, American Association of Petroleum geologists Memoir 3, pp. 90–125.

Rebollar, C. J., L. Quintanar, R. R. Castro, S. M. Day, J. Madrid, J. N. Brune, L. Astiz, and F. L. Vernon (2001), Source characteristics of a 5.5 magnitude earthquake that occurred in the transform fault system of the Delfín basin in the Gulf of California, Bull. Seism. Soc. Am., 91(4), 781–791.

Ritsema, J., and H. van Heijst (2000), New seismic model of the upper mantle beneath Africa, Geology, 28(1), 63–66.

Thatcher,W., and J. N. Brune (1973), Surface waves and crustal structure in the Gulf of California region, Bull. Seismol. Soc. Am., 63(5), 1689–1698.

Van der Lee, S. and A. Frederiksen, (2005), Surface wave tomography applied to North American upper mantle, in Seismic Herat, Array Análisis of Broadband Seismograms, eds, A. Levander and G. Nolet, Geophysical Monograph Series, 157, ISBN-13:978-0-87590-422-1, pp 67-80.

Date	Origin time	Latitude	Longitude	Depth (km)	Magnitude	ID
20021003	16:08:29	23.32	-108.53	10	6.5 M_w	eq1
20021029	14:16:54	34.80	-116.27	4	4.8 M_L	eq2
20021210	21:04:00	32.23	-115.80	7	4.8 M_L	eq3
20030207	10:34:04	31.63	-115.51	7	5.0 M_L	eq4
20030222	12:19:10	34.31	-116.85	1	5.2 M_w	eq5
20030312	23:41:32	26.56	-110.59	10	6.5 M_s	eq6
20030717	19:57:13	18.51	-107.13	10	6.0 M_w	eq7
20030825	23:24:59	18.54	-106.69	10	5.8 M_w	eq8
20031112	04:54:56	28.97	-113.22	10	5.6 M_w	eq9
20040209	01:24:40	24.90	-112.39	10	5.5 M_w	eq10
20040209	09:03:47	24.81	-112.51	10	5.4 M_w	eq11
20040218	10:59:19	23.64	-108.82	10	5.9 M_w	eq12
20040615	22:28:48	32.33	-117.92	10	5.3 M_L	eq13
20040714	00:53:52	33.71	-116.06	12	4.0 M_L	eq14
20040822	01:25:12	32.34	-115.22	6	4.2 M_L	eq15
20040830	05:35:16	29.52	-116.55	10	5.2 M_w	eq16
20040924	14:43:11	28.57	-112.72	10	5.9 M_w	eq17
20050106	00:02:21	19.57	-109.11	10	5.7 M_w	eq18
20050222	19:15:49	25.67	-109.97	10	5.5 M_w	eq19
20021123	02:33:01	18.47	-106.39	33	5.4 M_w	eq20
20021123	02:53:10	18.56	-106.48	33	5.4 M_w	eq21
20030415	08:21:17	25.03	-109.43	10	5.5 M_w	eq22
20030702	05:11:34	22.90	-108.19	10	5.6 M_w	eq23
20030811	01:17:53	18.35	-106.04	10	5.7 M_w	eq24
20050508	17:07:35	20.35	-109.19	10	5.9 M_w	eq25
20050605	08:28:50	23.67	-108.37	10	5.7 M_w	eq26
20050612	15:41:46	33.53	-116.57	14	5.2 M_w	eq27
20050616	20:53:26	34.06	-117.01	11	4.9 M_w	eq28
20050626	11:27:42	23.95	-108.69	10	4.7 m_b	eq29
20050627	11:35:45	18.78	-107.30	20	6.2 M_w	eq30

Table 1. List of Earthquakes used in the study. Their locations and magnitudes are from the NEIC catalogue.

Figure 1. Location map showing the events analyzed in this study, the NARS-Baja stations and gridded bathymetry in and around the Gulf of California. Source to receiver paths for 30 regional earthquakes (black solid dots) analyzed in this study. When available, Harvard moment tensor solutions are also plotted. Black solid triangles are the NARS-BAJA stations, whereas the open triangles are the RESBAN stations. The open circles indicate the main depositional basins in the Gulf of California: AB = Alarcon basin; DB = Delfín basin, composed of the Upper and Lower Delfín basins; FB = Farallon basin; GB = Guaymas basin; PB = Pescadero basin; TB = Tiburón basin; WB = Wagner basin; MF = Magdalena fan; EPR = East Pacific Rise; RT = Rivera Transform fault; IAG = Isla Angel de la Guarda; TI = Tiburón Island.

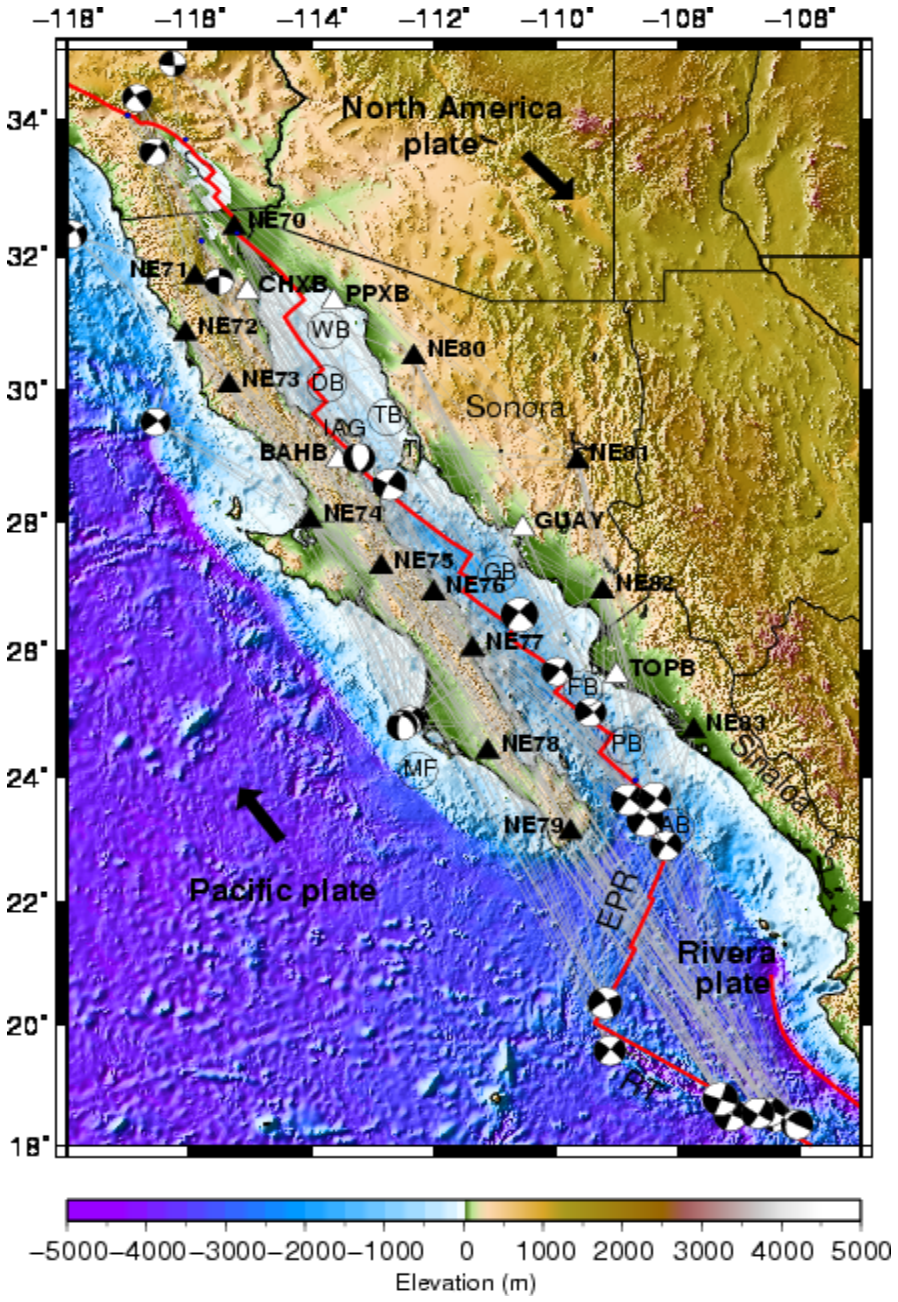

Figure 2. Raw data vertical component of the event eq12 listed in Table 1.

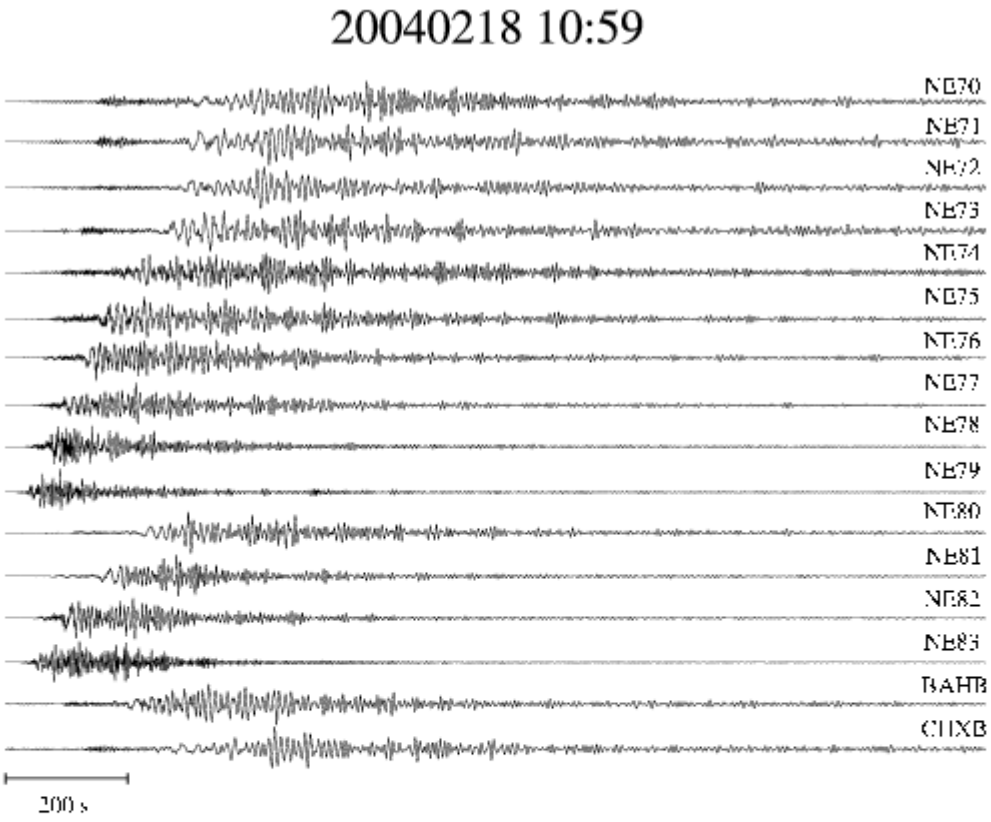

Figure 3. Examples of dispersion curves relative to events located at the mouth of the Gulf in the Alarcon Basin and along the Pescadero Transform fault (eq1 and eq12, top plots), along the Rivera Transform fault (eq8 and eq20 middle plots) and on the Pacific side of Baja California peninsula (eq10 and eq11, bottom plots), respectively.

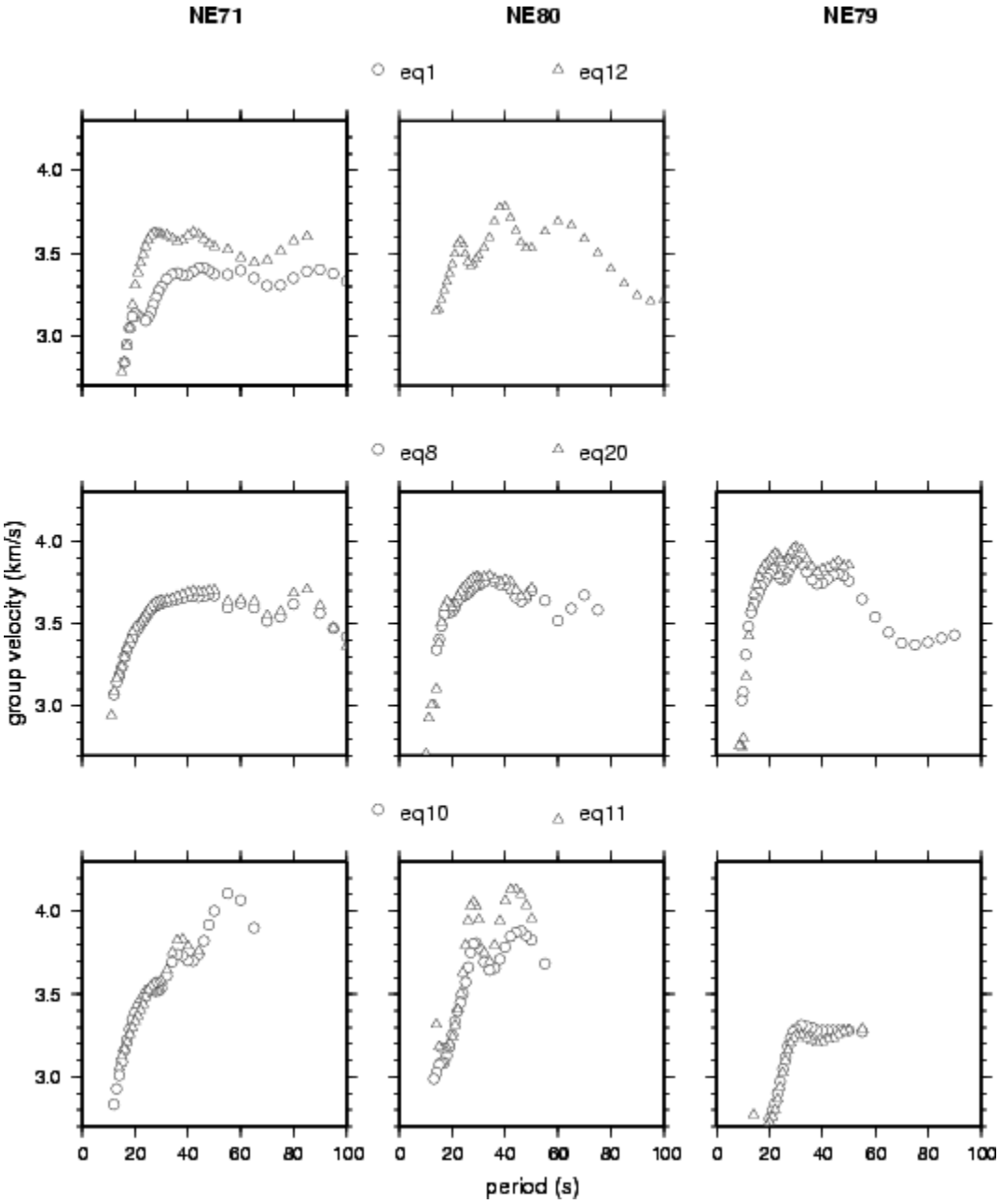

Figure 4. Tomographic model where open red dots represent each column whose crustal layers are taken from receiver functions studies by Ichinose et al. [1996], Lewis et al. [2002], Persaud et al., [2005], (green dots), and blue dots are from a reflection study by Gonz*ález-Fernández et al.* [2005]; outside the well sampled area, CRUST2.0 [*Bassin et al.*, 2000] is the reference model and for all the columns IASP91 is the used starting model for the mantle down to 500 km.

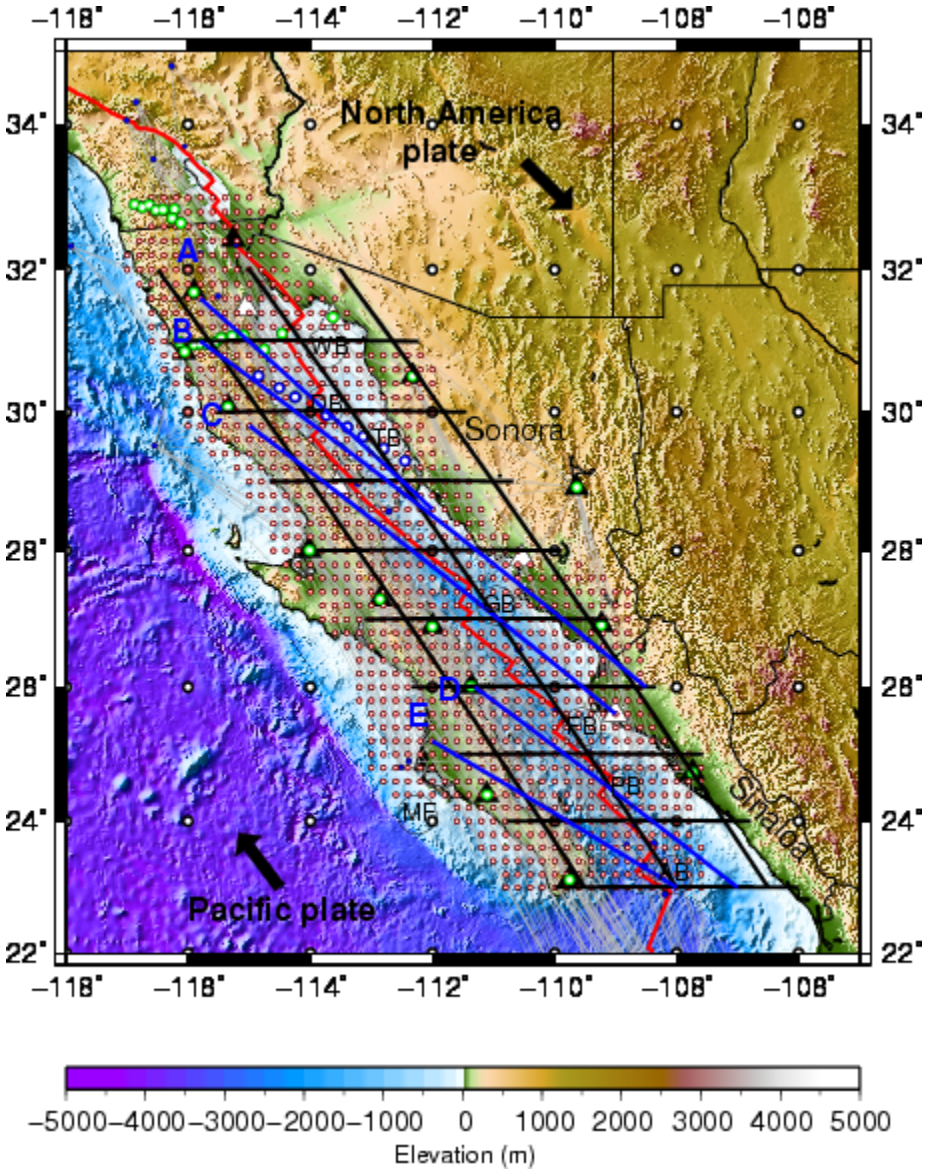

Figure 5. Left panels: Dispersion curves at latitudes of 23, 25 and 27°N are shown. Different colours refer to different longitudes. Dots and solid lines are the measured and predicted group velocities respectively. Central and right panels: shear wave velocity models used as initial models (central panels) and resulting from the inversion (right panels) of group velocities shown in the left panels.

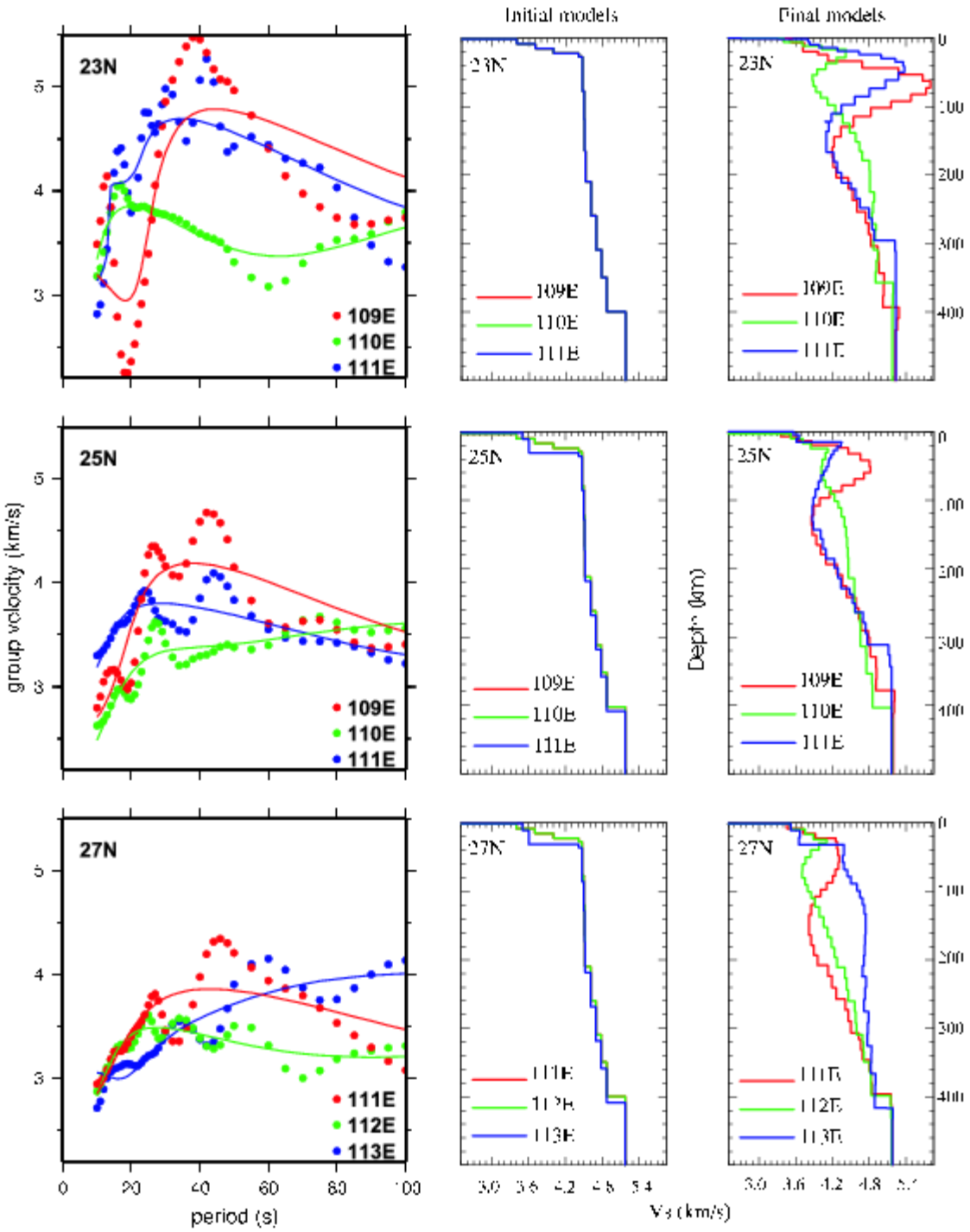

Figure 6a. Shear-wave velocity cross-sections roughly perpendicular to the main ridge axes (Figure 4). A: cross-section perpendicular to the Delfín basin; B: cross-section perpendicular to the Tiburón basin; C: cross-section perpendicular to the Guaymas basin; D: cross-section perpendicular to the Pescadero basin; E: cross-section perpendicular to the Alarcon basin.

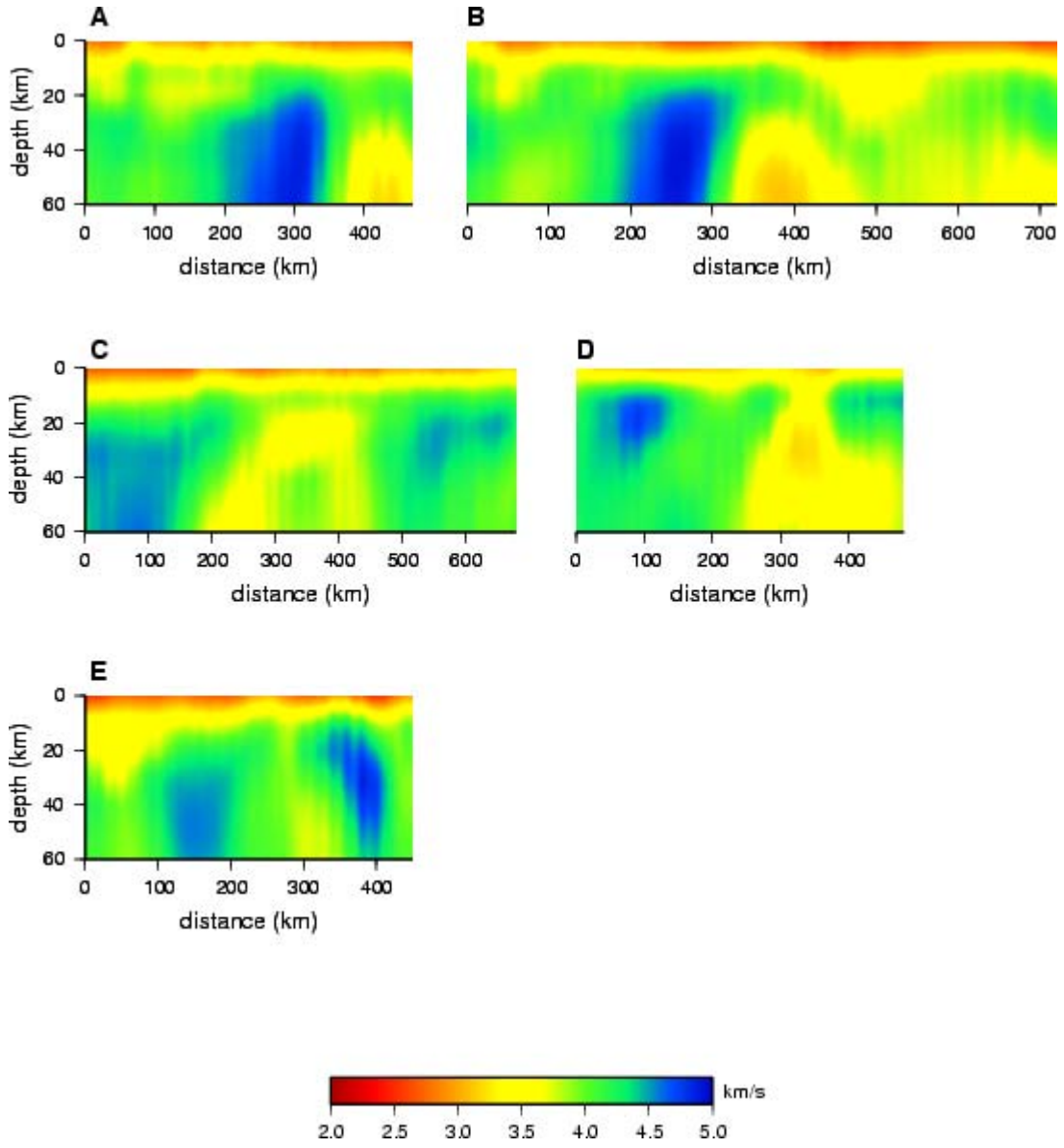

Figure 6b. Shear-wave velocity cross-sections crossing Baja California and the Gulf at different latitudes . See Figure 4 for the location of the cross-sections.

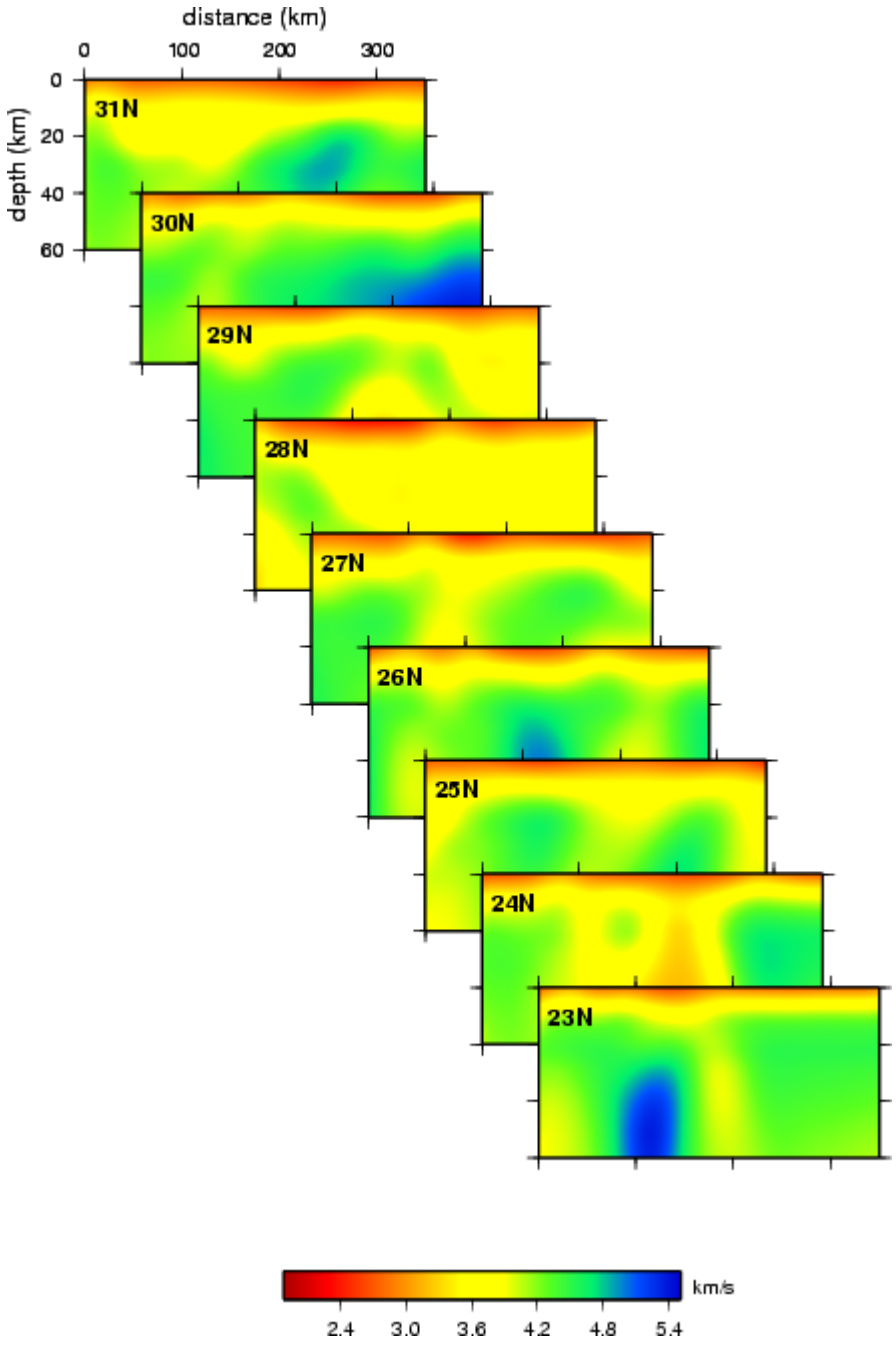

Figure 6c. Shear-wave velocity cross-sections parallel to the Gulf axis with a NW-SE orientation. W: western cross-section along Baja California; M: mid-Gulf cross-section; E: eastern cross-section along Sonora and Sinaloa regions.

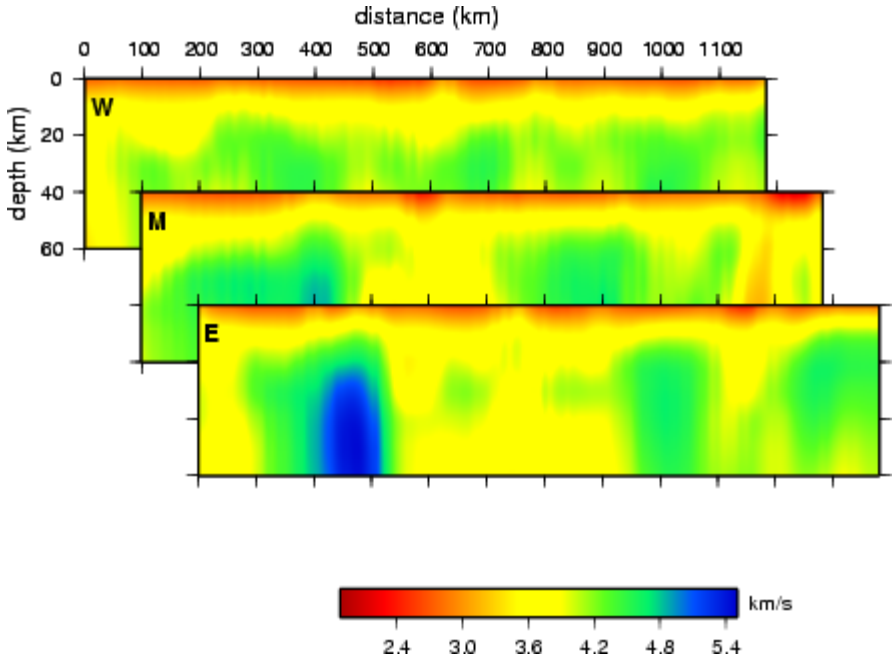

Figure 7. Comparison of the tomographic images of the sediment and crustal thickness between the initial model and the model obtained from the inversion.

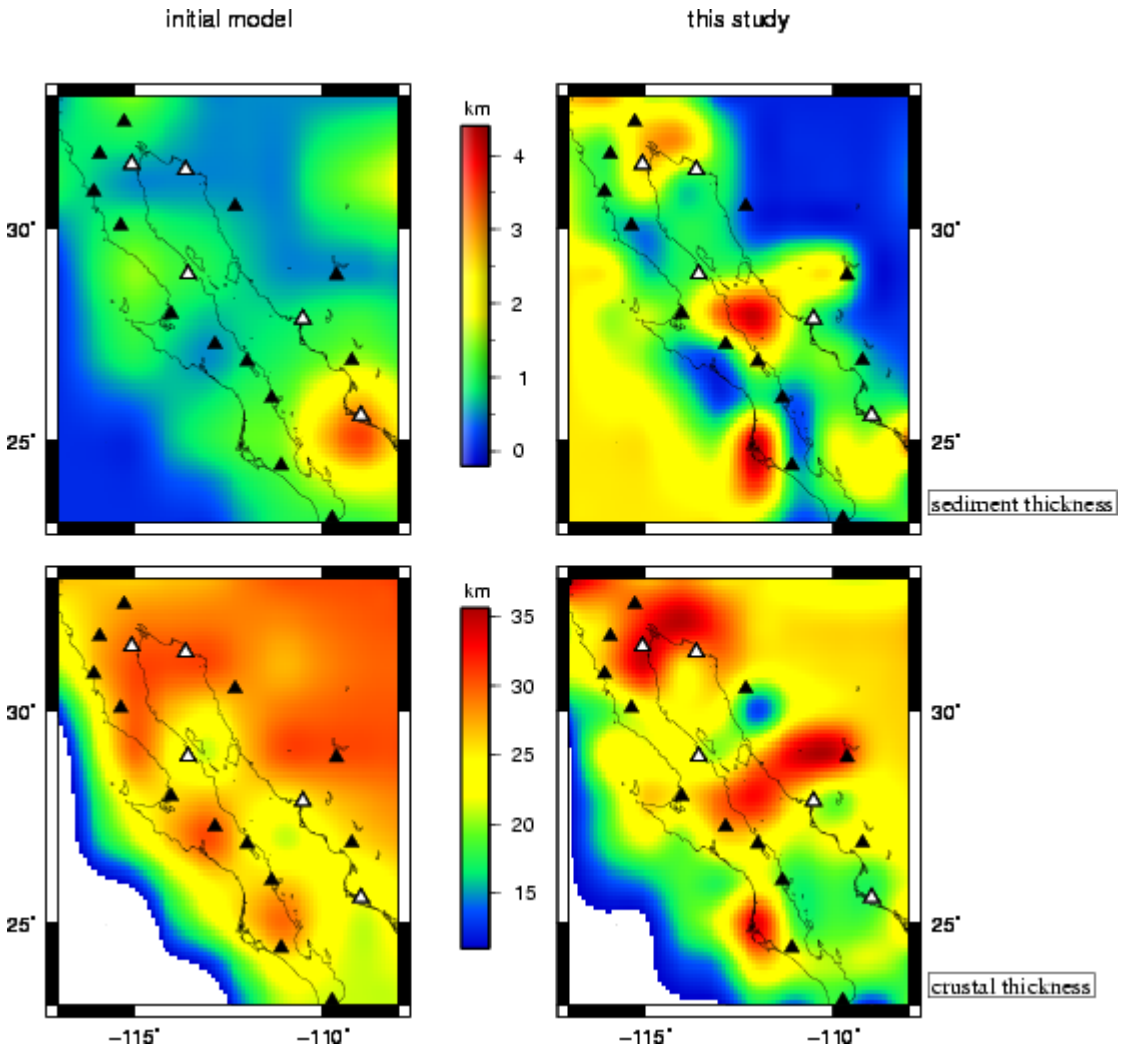

Figure 8. Tomographic maps of the shear wave velocities for the crust and upper mantle as from the initial model (left panels) and the inversion (right panels).